Goos-Hänchen shift at a temporal boundary

Sergey A. Ponomarenko, Junchi Zhang, and Govind P. Agrawal

Phys. Rev. A **106**, L061501 — Published 15 December 2022

DOI: 10.1103/PhysRevA.106.L061501

Goos-Hänchen shift at a temporal boundary

Sergey A. Ponomarenko,[1,2,*] Junchi Zhang,[3] and Govind P. Agrawal[3,4]

[1] *Department of Electrical and Computer Engineering, Dalhousie University, Halifax, Nova Scotia, B3J 2X4, Canada*

[2] *Department of Physics and Atmospheric Science, Dalhousie University, Halifax, Nova Scotia, B3H 4R2, Canada*

[3] *The Institute of Optics, University of Rochester, Rochester, New York, 14627 USA*

[4] *Laboratory for Laser Energetics, University of Rochester, Rochester, New York, 14623 USA*

(Dated: November 29, 2022)

We discover a pronounced temporal shift of the peak of an optical pulse upon total internal reflection of the pulse from a sharp temporal boundary propagating in a homogeneous, isotropic, weakly dispersive linear medium. We derive an analytical expression for this shift and juxtapose the discovered effect to the spatial Goos-Hänchen shift occurring on reflection of a beam from an interface separating two homogeneous, isotropic, conservative linear media. In particular, we show that, in contrast to the spatial shift, the sign of the temporal shift is dictated by that of the group velocity mismatch between the pulse and the temporal boundary, implying the possibility of a delay or advancement of the pulse upon reflection. Our analytical results, which are in excellent agreement with our numerical simulations, shed light on fundamental aspects of the interaction of wave packets with temporal boundaries in material media.

PACS numbers:

The celebrated Goos–Hänchen (GH) effect corresponds to a shift of the beam center relative to its geometrical-optics prediction upon total internal reflection of a light beam from a spatial boundary separating two homogeneous optical media [1]. The GH effect takes place in frustrated total internal reflection as well [2, 3]. The significance of the GH effect is twofold. On the one hand, the GH shift heralds the wave nature of light and underscores inadequacy of a purely geometrical-optics description of light beams in the situations involving light-matter interactions. On the other hand, the GH effect is germane to wave packets in material media of any nature. Indeed, the optical GH effect [4, 5] has been discovered and documented for an impressive variety of natural materials, including glasses [6], noble metals [7, 8], superconductors [9], nematic liquid crystals [10], graphene [11], nonlinear materials [12, 13], as well as for metamaterials [14–17]. Besides photonics, the GH effect has been discovered for wave packets in atom optics [18], electron wave packets [19, 20], neutrons [21], spin waves [22], and even quantized matter waves [23]. In addition, GH shifts were observed in acoustics [24, 25] and are predicted to occur in seismology [26].

While light-matter interactions at spatial interfaces have been extensively studied, the behavior of light in time-varying media has attracted attention only recently [27, 28], triggered by the concept of a temporal boundary (TB) [29] and the exploration of light transmission and reflection through the TB [30]. To date, many of the concepts and phenomena associated with light-matter interactions at the spatial interface have been extended to the time domain, including total internal reflection [31], waveguides [32, 33], the effective medium theory [34], anti-reflection coatings [35], Fabry-Perot cavities [36, 37], photonic crystals [38–40], and Brewster angle [41]. In addition, anomalous light statistics associated with the TB soliton formation [42], extreme energy transformations at non-Hermitian TBs [43], and temporal aiming [44] have been discovered that have no direct spatial analogues.

In this context, a fundamental question can be raised: Does there exist a counterpart of a spatial GH effect taking place at the TB, and if so, what are the key parameters of a time-varying medium supporting such an effect?

In this Letter, we show that even in the most basic setting of a homogeneous, isotropic, weakly dispersive linear medium, a pronounced temporal shift of the peak of an optical pulse can occur upon total internal reflection (TIR) of the pulse from a sharp TB propagating in such a medium. We refer to this phenomenon as a Goos-Hänchen shift at a temporal boundary (GHSTB). In a parameter regime accessible in typical silica-glass fibers, the discovered GHSTB is much larger than its spatial counterpart at the interface separating two homogeneous, isotropic, lossless linear media. We also demonstrate that unlike its spatial analogue in the same conditions, the GHSTB can be either positive (delay) or negative (advancement) depending on the sign of the group velocity mismatch between the pulse and the TB. We stress that our results link two active areas of research: the physics of wave-matter interactions at interfaces and photonics of time-varying media.

As the GH effect at the TB is intimately related to TIR, we start by ensuring that the conditions for temporal TIR, elucidated in [31], are met. To this end, we consider a sharp, step-like TB moving at a speed of v_b in a weakly dispersive linear medium. The TB introduces a refractive index jump $\Delta n(t) = \Delta n\theta(t - t_b - z/v_b)$, where Δn and t_b are the magnitude and temporal po-

sition of the jump, respectively, and $\theta(x)$ is the Heaviside step function. The envelope $\mathcal{E}$ of the electric field $E(t,z)=\mathcal{E}(t,z)e^{i(\beta_0 z-\omega_0 t)}$ of a pulse with the carrier frequency ω_0 obeys a quasi-monochromatic wave equation,

$$i\partial_z\mathcal{E}+i\beta_1\partial_t\mathcal{E}-\tfrac{1}{2}\beta_2\partial_{tt}^2\mathcal{E}+k_0\Delta n\theta(t-t_b-z/v_b)\mathcal{E}=0, \quad (1)$$

where β_1 and β_2 are the usual notations for the inverse of the group velocity and its dispersion. Transforming to the TB's reference frame by changing variables as $\zeta=z$, $\tau=t-t_b-z/v_b$, we arrive at

$$i\partial_\zeta\mathcal{E}+i\Delta\beta_1\partial_\tau\mathcal{E}-\tfrac{1}{2}\beta_2\partial_{\tau\tau}^2\mathcal{E}+k_0\Delta n\theta(\tau)\mathcal{E}=0. \quad (2)$$

Here $\Delta\beta_1=\beta_1-v_b^{-1}$ is (inverse) group-velocity mismatch between the pulse and the TB.

At this point, we clarify the distinct roles of group-velocity dispersion and group-velocity mismatch in the light-matter interaction at the TB. With this objective, we make a gauge transformation, $\mathcal{E}=Ue^{i(\nu\tau+\alpha\zeta)}$, and choose ν and α to eliminate the convective (linear) term on the left side of Eq. (2), thereby reducing the latter to

$$i\partial_\zeta U-\tfrac{1}{2}\beta_2\partial_{\tau\tau}^2U+k_0\Delta n\theta(\tau)U=0, \quad (3)$$

for $\nu=-\Delta\beta_1/\beta_2$ and $\alpha=\Delta\beta_1^2/2\beta_2$. Eq. (3) is mathematically equivalent to the Schrödinger equation with an effective potential barrier $k_0\Delta n\theta(\tau)$.We notice that in the reference frame of the TB, the barrier is independent of the spatial coordinate, thereby implying the existence of the refractive index jump in time only. This jump is independent of the group velocity mismatch. Hence the latter cannot affect the energy distribution between the transmitted and reflected waves, which is governed by the interplay of the refractive-index jump and group-velocity dispersion [45]. However, group-velocity mismatch does affect kinematics of the reflected pulse, and hence the magnitude of the GHSTB incurred during TIR of a relatively long incident pulse at the TB.

Next, we seek plane-wave solutions to Eq. (3) in the form

$$U=\begin{cases} e^{i(q\zeta-\Omega_i\tau)}+Re^{i(q\zeta-\Omega_r\tau)}, & \tau<0,\\ Te^{i(q\zeta-\Omega_t\tau)}, & \tau>0,\end{cases} \quad (4)$$

where R and T are, in general, complex reflection and transmission amplitudes and the subscripts i, r, and t stand for incident, reflected and transmitted waves. In the reference frame of the TB, the wave number q is the same for the three waves because translational invariance implies linear momentum conservation in this reference frame. On substituting from Eq. (4) into (3) we can determine the frequencies (relative to the carrier) of the transmitted and reflected waves and by applying the boundary conditions to the TB, we can find the complex transmission and reflection amplitudes (see Supplemental Material [45] for details). We find that $\Omega_r=-\Omega_i$ and

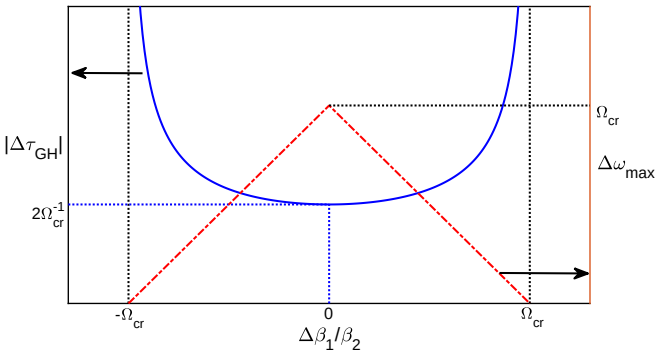

FIG. 1: Qualitative behavior of the magnitude of the GHSTB (solid blue curve) and maximum available bandwidth (dashed red lines) as a function of $\Delta\beta_1/\beta_2$. Dotted lines mark the limiting values.

$\Omega_t=\sqrt{\Omega_i^2-\Omega_{\rm cr}^2}$, where the critical frequency for TIR is given by

$$\Omega_{\rm cr}=\sqrt{2k_0\Delta n/\beta_2}. \quad (5)$$

It follows that any incident wave with the frequency $|\Omega_i|\le\Omega_{\rm cr}$ is totally internally reflected from the TB (because Ω_t becomes purely imaginary). Moreover, it can be shown [45] that the reflection amplitude is unimodular such that $R_{\rm TIR}=e^{i\phi_{\rm TIR}}$, where the TIR phase is given by

$$\phi_{\rm TIR}(\Omega_i)=2\arctan(\sqrt{\Omega_{\rm cr}^2/\Omega_i^2-1}). \quad (6)$$

For a pulse to undergo TIR, all frequency components within its bandwidth $\Delta\omega_B$ must satisfy the condition $|\Omega_i|\le\Delta\omega_B$, which translates to the constraint [45]

$$\Delta\omega_B\le\Delta\omega_{\rm max}=\Omega_{\rm cr}-|\Delta\beta_1/\beta_2|. \quad (7)$$

As a final step of our derivation, we Fourier synthesize all frequency components of the pulse to infer that a totally internally reflected pulse maintains its shape, acquires a global phase shift, and, most important, exhibits a shift of its center position given by the expression [45]

$$\Delta\tau_{\rm GHSTB}=\partial_{\Omega_i}\phi_{\rm TIR}|_{\Omega_i=\Delta\beta_1/\beta_2}. \quad (8)$$

On substituting from Eq. (6) into (8) we obtain, after elementary algebra, the following elegant analytical expression for the GHSTB of the pulse:

$$\Delta\tau_{\rm GHSTB}=\frac{2\,{\rm sign}(\Delta\beta_1)}{\sqrt{\Omega_{\rm cr}^2-\Delta\beta_1^2/\beta_2^2}}. \quad (9)$$

Prior to analyzing our main result, we note that the validity of Eq. (9) requires that the reflected pulse shape remain intact, which mathematically translates to [45]

$$|\Delta\tau_{\rm GHSTB}|\ll\sqrt{\frac{8}{\Delta\omega_B}\left|\frac{\beta_2}{\Delta\beta_1}\right|}. \quad (10)$$

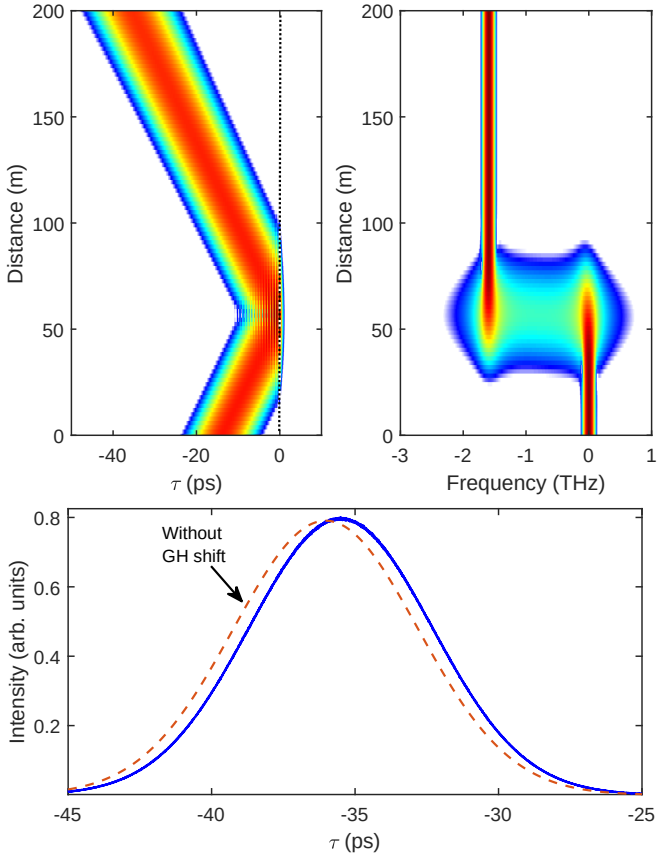

FIG. 2: Temporal and spectral evolution of a 6-ps-wide Gaussian pulse undergoing TIR in a 200-m-long fiber using $\beta_2 = 0.05$ ps^2/m, $\Delta\beta_1 = 0.25$ ps/m, and $k_0\Delta n = 1$ m^{-1}. The bottom part compares intensity profile of the reflected pulse to a pulse without the GHSTB.

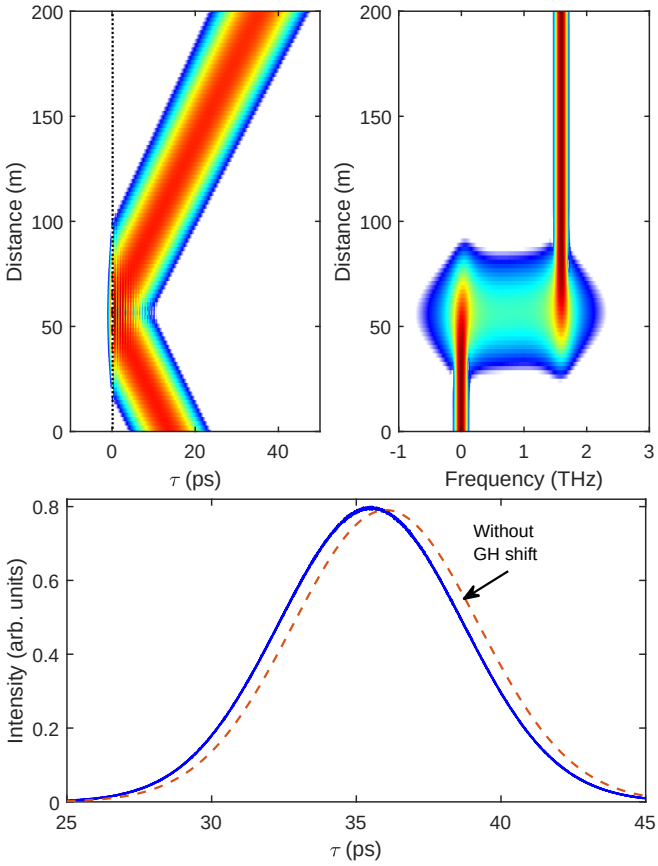

FIG. 3: Temporal and spectral evolution of a 6-ps-wide Gaussian pulse undergoing TIR under the conditions of Fig. 2 except for a change in the sign of group-velocity mismatch: $\Delta\beta_1 = -0.25$ ps/m.

Eqs. (7), (9) and (10) determine the magnitude and sign of the GHSTB and establish the range of applicability of our main analytical result.

We notice that Eq. (9) predicts extremely large shifts as $|\Delta\beta_1/\beta_2|$ approaches the critical frequency. However, the bandwidth of any reflected pulse shrinks to zero in the same limit, as indicated by Eq. (7). It follows that arbitrarily large values of the GHSTB are unattainable in practice. We illustrate this point in Fig. 1, where we sketch the magnitude of the GHSTB (solid curve) and the maximum bandwidth $\Delta\omega_{\max}$ (tilted dashed lines) as functions of $\Delta\beta_1/\beta_2$.

To provide a realistic estimate of the GHSTB, we use the parameter values appropriate for optical fibers: $\beta_2 = 0.05$ ps^2/m and $\Delta\beta_1 = 0.25$ ps/m. We choose $k_0\Delta n = 1$ m^{-1}, which corresponds to a refractive-index change at the TB of less than 10^{-6} at $\lambda_0 = 1\,\mu$m. We can infer at once from Eq. (9) that $\Delta\tau_{\rm GHSTB} = 0.516$ ps. To verify our analytical result, we performed numerical simulations based on Eq. (2) with an incident Gaussian pulse of 6-ps FWHM at $z = 0$. The peak of the pulse is initially ahead of the TB by 14 ps. Figure 2 shows the temporal and spectral evolution of the pulse undergoing TIR in a 200-m-long fiber. Note the large spectral shift occurring around 50 m when the pulse hits the TB. The bottom part compares the intensity profile of the reflected pulse to a "mirrored" pulse, obtained by propagating the incident pulse to the point of comparison with the sign of group-velocity mismatch reversed. We can infer from the figure that the peak of the reflected pulse is indeed delayed relative to that of the mirror image. The numerically evaluated delay of 0.524 ps agrees well with our analytical prediction; we attribute a slight discrepancy to numerical roundoff errors. The magnitude of the GHSTB is 8.6% of the input pulse's width. This value should be contrasted to a tiny spatial GH shift ($\sim 1\ \mu$m) occurring at a spatial interface separating two homogeneous linear media ($< 1\%$ of the beam width).

Next, it follows at once from Eq. (9) that the sign of the GHSTB is governed by that of $\Delta\beta_1$, implying that the peak of the reflected pulse is either delayed or advanced in time, depending on whether the TB overtakes the pulse, ($\Delta\beta_1 > 0$), or the pulse catches up to the TB ($\Delta\beta_1 < 0$). This situation stands in stark contrast

to the textbook GH shift at a spatial boundary between two lossless isotropic media, which always corresponds to a delay [46]. We note, though, that the sign of the spatial GH shift can be altered if one of the media is absorbing [47–49]), amplifying [50], or possesses spatial dispersion [51].

To verify the dependence of the GHSTB on the sign of the group-velocity mismatch, we show in Fig. 3 the evolution of the same Gaussian pulse under identical conditions to those in Fig. 2, except for the sign of group-velocity mismatch: $\Delta\beta_1 = -0.25$ ps/m. A comparison of Figs. 2 and 3 reveals that the GHSTB flips sign as well, in complete agreement with our predictions. We note that the delay or advancement of the peak of the reflected pulse is captured in the spectrum by a red or blue spectral shift triggered by TIR. We also verified with numerical simulations the range of applicability of our analytical results (see Fig.1 of the Supplemental material [45]) and near independence of the GHSTB on the pulse shape—see Fig. 2 of the Supplemental Material [45], where we exhibit the spectral and temporal evolution for the TIR of a secant hyperbolic pulse.

We observe that the GHSTB, visible in Figs. 2 and 3, appears smaller relative to the width of the pulse, compared to the value expected relative to the width of the incident pulse. This is because the incident pulse broadens before it arrives at the location where we compare the reflected and "mirrored" pulses. In this connection, we may inquire about the conditions under which the relative GHSTB is maximized. We conjecture that the incident pulse has to be delayed relative to the TB just enough to ensure that the evolution of the incident and reflected pulses is symmetric with respect to the point of contact with the TB. Further numerical analysis reveals that we can maximize the GHSTB relative to the width of the reflected pulse as a function of the dimensionless quantity $\Omega_{\rm cr} t_p$. For our numerical simulations, we consider a linear medium with $\beta_2 = 0.05$ ps^2/m and $\Delta\beta_1 = 0.3$ ps/m. The refractive index jump at the TB is such that $k_0\Delta n = 1.79$ m^{-1}. The TB is delayed by 3.6 ps with respect to the peak of a Gaussian pulse of 2-ps FWHM. In Fig. 4, we exhibit the spectral and temporal evolution of the optimized pulse under TIR and compare the reflected and "mirrored" pulses at $z = 24.2$ m; the corresponding maximum GHSTB is 23% of the incident pulse's width. We can infer from Fig. 4 that such a pronounced GHSTB corresponds to a rather symmetric evolution (both in time and frequency) of the incident pulse under TIR, thus validating our intuition.

Finally, we discuss how a sharp temporal boundary, which is a prerequisite for the observation of the GHSTB, can be engineered. Previous proposals relied, for the most part [27, 31], either on generating a microwave front with the aid of electro-optical modulation or on producing a moving TB using cross-phase modulation by a soliton-like pulse through the Kerr nonlinearity of

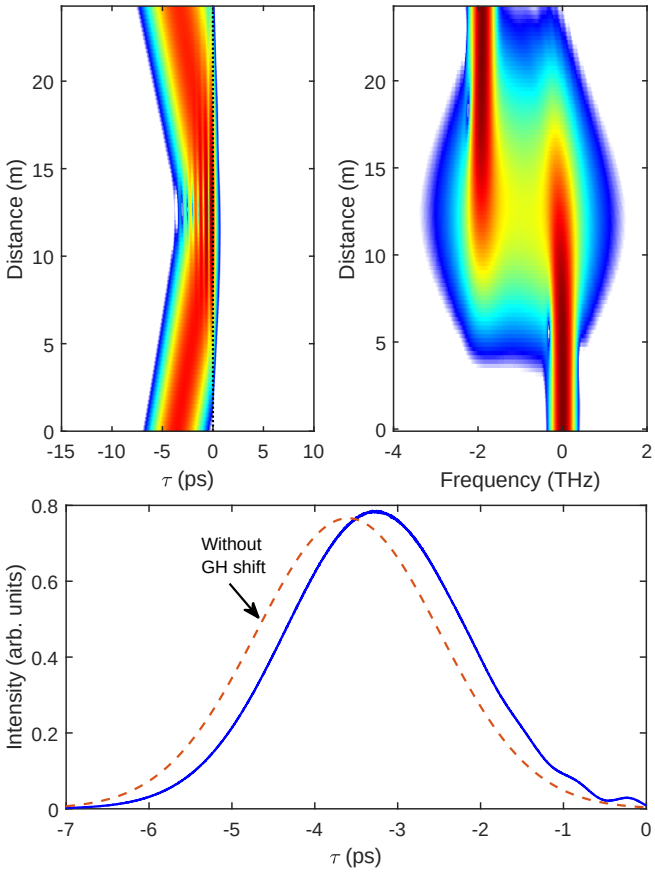

FIG. 4: Optimization of the GHSTB. Temporal and spectral evolution of a 2-ps-wide Gaussian pulse undergoing TIR in a medium with $\beta_2 = 0.05$ ps^2/m, $\Delta\beta_1 = 0.3$ ps/m, and $k_0\Delta n = 1.79$ m^{-1}. The bottom part compares intensity profile of the reflected pulse to a pulse without the GHSTB.

the medium. Unfortunately, both approaches suffer from potential drawbacks. The microwave front can only be generated in a waveguide over a very limited axial distance, whereas creating a high-intensity kink-like profile in a nonresonant medium can be a tall order, considering relative weakness of the Kerr nonlinearity. To overcome these hurdles, we propose to dope a fiber with resonant impurities, such as atom defects or quantum dots, and launch a quasi-continuous wave with its carrier frequency close to the impurity resonance into the doped fiber. Provided the transverse (coherence) relaxation time of the medium is much shorter than its longitudinal (population inversion) relaxation time, an optical kink is naturally formed over a short propagation distance for both homogeneously [52] and inhomogeneously [53] broadened collection of impurities. This kink can serve as a sharp temporal boundary for a weak probe pulse, whose frequency is detuned far from the impurity resonance, through the cross-phase modulation mediated by the Kerr nonlinearity of the host medium. We stress that the advantage of our proposal is in resonant enhancement of the index

change Δn. We also point out that the group velocity mismatch can be controlled by adjusting either the probe wavelength or the detuning from the impurity resonance.

In conclusion, we introduced the concept of a Goos-Hänchen shift at a temporal boundary moving in a homogeneous, weakly dispersive linear medium. We have derived a simple analytical expression for the GHSTB and showed that its sign depends on the sign of group velocity mismatch between the pulse and the temporal boundary. Although, formally speaking, the mathematical expression for GHSTB, Eq. (8), in terms of the derivative of a reflection coefficient with respect to frequency is reminiscent of a Newton–Wigner time delay, which occurs on scattering of a pulse from interfaces [54–56] or structured media [57], the discovered shifts are caused by TIR at a TB. Thus, the physics of GHSTB is intimately linked to the Goos-Hänchen effect at the temporal boundary. Our results forge a link between the physics of GH effect and photonics of time-varying media. Just as the spatial GH effect has found numerous applications, from optical heterodyne sensing [58] to the design of micrometer-size surface-resonance waveguide devices [59], we anticipate our results to open new avenues in the design and manipulation of time metamaterials. We note that measuring the discovered GHSTBs presents an open challenge at the moment. Facing this challenge will trigger novel fundamental developments in photonics of time-varying media.

The authors acknowledge financial support from Natural Sciences and Engineering Research Council of Canada (RGPIN-2018-05497) and U.S. National Science Foundation (ECCS-1933328).

* serpo@dal.ca

[1] F. Goos and H. Hänchen, Ein neur und fundamentaler Versuch zur Totalreflexion, Ann. Phys. (Leipzig) **436**, 333 (1947).

[2] A. Haibel, G. Nimtz, and A. A. Stalhofen, Frustrated total reflection: The double-prizm revisited, Phys. Rev. E **63**, 047601 (2001).

[3] X. Chen, X-J Lu, P-L Zhao, and Q-B Zhu, Energy flux and Goos–Hänchen shift in frustrated total internal reflection, Opt. Lett. **37**, 1526 (2012).

[4] K. Y. Bliokh, I. V. Shadrirov, and Y. Kivshar, Goos–Hänchen and Imbert-Fedoryov shifts of polarized vortex beams, Opt. Lett. **34**, 389 (2009).

[5] 3. K. Y. Bliokh and A. Aiello, Goos–Hänchen and Imbert-Fedorov beam shifts: an overview, J. Opt. **15**, 014001 (2013).

[6] F. Bretanaker, A. Le Floch, and L. Dutriaux, Direct measurement of the optical Goos–Hänchen effect in lasers, Phys. Rev. Lett. **68**, 931 (1992).

[7] X. Yin, L. Hesselink, Z. Liu, N. Fang, and X. Zhang, Large positive and negative lateral optical beam displacements due to surface plasmon resonance Appl. Phys. Lett. **85**, 372 (2004).

[8] X. Yin and L. Hesselink, Goos–Hänchen shift surface plasmon resonance sensor, Appl. Phys. Lett. **89**, 261108 (2006).

[9] S.-Y. Lee, A. Goussev, O. Georgiou, G. Gligoric, and A. Lazarides, Sticky Goos-Hänchen effect at normal/superconductor interface, EPL **103**, 20004 (2013).

[10] M. Peccianti, A. Dyadyusha, M. Kaczmarek, and G. Assanto, Tunable refraction and reflection of self-confined light beams, Nat. Phys. **2**, 737 (2006).

[11] M. Shah, A. Akbar, N. A. Khan, Q. Zaman, S. Iqbal, W. Ali, M. Javed, and M. Shah, Quantization of Goos–Hänchen shift in monolayer graphene under partial and total internal reflection conditions, J. Opt. Soc. Am. B **39**, 1082 (2022).

[12] O. Emile, T. Galstyan, A. Le Foch, and F. Bretenaker, Measurement of the nonlinear Goos–Hänchen effect for Gaussian optical beams, Phys. Rev. Lett. **75**, 1511 (1995).

[13] B. M. Jost, A. A. R. Al-Rashed, and B. E. A. Saleh, Observation of Goos–Hänchen effect in a phase conjugate mirror, Phys. Rev. Lett. **81**, 2233 (1998).

[14] P. R. Berman, Goos–Hänchen shifts in negatively refracting media, Phys. Rev. E **66**, 067603 (2002).

[15] J. He, J. Yi, and S. He, Giant negative Goos–Hänchen shifts for a photonic crystal with a negative effective index, Opt. Express **14**, 3024 (2006).

[16] S. Longhi, G. D. Valle, and K. Staliunas, Goos–Hänchen shift in complex crystals, Phys. Rev. A **84**, 042119 (2011).

[17] I. Soboleva, V. Moskalenko, and A. Fedyanin, Giant Goos-Hänchen effect and Fano resonance at photonic crystal surfaces, Phys. Rev. Lett. **108**, 123901 (2012).

[18] J. Huang, Z. Duan, H. Ling, and W. Zhang, Goos-Hänchen shifts in atom optics, Phys. Rev. A **77** 063608 (2008).

[19] C. W.J. Beenakker, R. A. Sepkhanov, A.R. Akhmerov, and J. Tworzydlo, Quantum Goos-Haänchen effect in graphene, Phys. Rev. Lett. **102**, 146804 (2009).

[20] Z. Wu, F. Zhai, F. M. Peeters, H. Q. Xu, and K. Chang, Valley-Dependent Brewster Angles and Goos-Hänchen Effect in Strained Graphene, Phys. Rev. Lett. **106**, 176802 (2011).

[21] V. O. De Haan, J. Plomp, T. M. Rekveldt, W. H. Kraan, A. A. van Well, R. M. Dalgliesh, and S. Langridge, Observation of the Goos-Hänchen shift with neutrons, Phys. Rev. Lett. **104**, 010401 (2010).

[22] Y. S. Dodoenkova, N.N. Dodoenkova, I. L. Lyubchanskii, M. L. Sokolovskyy, J. W. Kols, J. Romero-Vivas, and M. Krawczyk, Huge Goos-Hänchen effect for spin waves: A promising tool for study magnetic properties at interfaces Appl. Phys. Lett. **101**, 042404 (2012).

[23] S.-Y Lee, J. Le Deunff, M. Choi, and R. Ketzmerick, Quantum Goos-Hänchen shift and tunneling transmission at a curved step potential, Phys. Rev. A **89**, 022120 (2014).

[24] M. A. Breazeale and M. A. Torbett, Backward displacement of waves reflected from an interface having superimposed periodicity, Appl. Phys. Lett. **29**, 456 (1976).

[25] N. F. Declercq, J. Degrieck, and O. Leroy, The double-sided ultrasonic beam displacement, Appl. Phys. Lett. **85**, 4234 (2004).

[26] Z. Wang, The influence of the Goos-Hänchen effect on seismic data processing and AVO in attenuating media, J. Appl. Geophys., **122**, 122 (2015).

[27] E. Galiffi, R. Torole, S. Yin, H. Li, S. Vezzoli, P. A. Huidobro, M.G. Silverinha, R. Sapienza, A. Alù, and J. B. Pendry, Photonics of time-varying media, Adv. Photon., **4**, 014002 (2022).

[28] J. Xu, W. Mai, and D. H. Werner, Generalized temporal transfer matrix method: a systematic approach to solving electromagnetic wave scattering in temporarily stratified structures, Nanophotonics., **11**, 1309 (2022).

[29] J.T. Medonça and P. K. Shukla, Time refraction and time reflection: two basic concepts, Phys, Scripta, **65**, 160 (2002).

[30] Y. Xiao, G. P. Agrawal, and D.N. Maywar, Reflection and transmission of electromagnetic waves at a temporal boundary, Opt. Lett. **39**, 574 (2014).

[31] B.P. Plansinis, W.R. Donaldson, and G. P. Agrawal, What is the temporal analog of reflection and refraction of optical beams? Phys. Rev. Lett. **115**, 183901 (2015).

[32] B.P. Plansinis, W.R. Donaldson, and G. P. Agrawal, Temporal waveguides for optical pulses, J. Opt. Soc. Am. B **33**, 1112, (2016).

[33] J. Zhou, G. Zhang, and J. Wu, Comprehensive study on the concept of temporal optical waveguides, Phys. Rev. A, **93**, 063847 (2016).

[34] V. Pacheco-Peña and N. Engheta, Effective medium concept in temporal metamaterials, Nanophotonics, **9**, 379 (2020).

[35] V. Pacheco-Peña and N. Engheta, Antireflection temporal coatings, Optica, **7**, 323 (2020).

[36] D. Ramaccia, A. Toscano, and F. Bilotti, Light propagation through metamaterial temporal slabs: reflection, refraction, and special cases, Opt. Lett. **45**, 5836 (2020).

[37] J. Zhang, W. R. Donaldson, and G. P. Agrawal, Time-domain Fabry-Perot resonators formed inside a dispersive medium, J. Opt. Soc. Am. B **38**, 2376 (2021).

[38] E. Lustig, Y. Sharabi, and M. Segev, Topological aspects of photonic time crystals, Optica **5**, 1390 (2018).

[39] Y. Sharabi, E. Lustig, and M. Segev, Disordered photonic time crystals, Phys. Rev. Lett. **126**, 163902 (2021).

[40] J. S. Martínez-Romero, O. M. Bacerra-Fuentes, and P. Halevi, Temporal photonic crystals with modulations of both permittivity and permeability, Phys. Rev. A **93**, 063813 (2016).

[41] V. Pacheco-Peña and N. Engheta, Temporal equivalent of the Brewster angle, Phys. Rev. B **104**, 214308 (2021).

[42] C. Liang, S. A. Ponomarenko, F. Wang, and Y. Cai, Temporal Boundary Solitons and Extreme Superthermal Light Statistics, Phys. Rev. Lett. **127**, 053901 (2021).

[43] H. Li, S. Yin, E. Galiffi, and A. Alù, Temporal parity-time symmetry for extreme energy transformations, Phys. Rev. Lett. **127**, 153903 (2021).

[44] V. Pacheco-Peña and N. Engheta, Temporal aiming, Light. Sci. Appl. **9**, 129 (2020).

[45] See Supplemental Material for details of our analytical derivations and supplementary figures.

[46] J. D. Jackson, *Classical Electrodynamics* (Wiley, 1999) 3rd Ed.

[47] E. Pfleghaar, A. Marseille, and A. Weis, Quantitative investigation of the effect of resonant absorbers on the Goos-Hännchen shift, Phys. Rev. Lett. **70**, 2281 (1993).

[48] L. G. Wang, M. Ikram, and M. S. Zubairy, Control of the Goos-Hänchen shift of a light beam via a coherent driving field, Phys. Rev. A **77**, 023811 (2008).

[49] Ziauddin, S. Qamar, and M. S. Zubairy, Coherent control of the Goos-Hänchen shift, Phys. Rev. A **81**, 023821 (2010).

[50] Ziauddin and S. Qamar, Gain-assisted control of Goos-Hänchen effect, Phys. Rev. A **84**, 053844 (2011).

[51] J. L. Birman, D. N. Patttanayak, and A. Puri, Prediction of a Resonance-Enhanced Laser-Beam Displacement at Total Internal Reflection in Semiconductors, Phys. Rev. Lett. **50**, 1664 (1983).

[52] S. A. Ponomarenko and S. Haghgoo, Self-similarity and optical kinks in resonant nonlinear media, Phys. Rev. A **82**, 051801(R), (2010).

[53] S. Haghgoo and S. A. Ponomarenko, Optical shocks in resonant media: The role of inhomogeneous broadening, Opt. Commun., **286**, 344 (2013).

[54] H. Kogelnik and H. P. Weber, Rays, stored energy and power flow in dielectric waveguides, J. Opt. Soc. Am. **64**, 174 (1974).

[55] P. Balcou and L. Durtiaux, Dual Optical Tunneling Times in Frustrated Total Internal Reflection, Phys. Rev. Lett. **78**, 851 (1997).

[56] A. Le Floch, O. Emile, G. Ropars, and G. P. Agrawal, Dynamics and detection of the Newton-Wigner time delays at interfaces using a swivelling method, Sci. Rep. **7**, 9083 (2017).

[57] M. Asano, K.Y. Bliokh, Y. P. Bliokh, A.G. Kofman, R. Ikuta, T. Yamamoto, Y. S. Kivshar, L. Yang, N. Imoto, S. Z. Özdemir, and F. Nori, Anomalous time delays and quantum weak measurements in optical microresonators, Nat. Commun. **7**, 13488 (2016).

[58] T. Hashimoto and T. Yoshino, Optical heterodyne sensor using the Goos-Hänchen shift, Opt. Lett. **14**, 913 (1989).

[59] G.-Y. Oh, D. G. Kim, and Y.-W. Choi, The characterization of GH shifts of surface plasmon resonance in a waveguide using the FDTD method, Opt Express **17**, 20714 (2009).